
CMS Analysis Note

The content of this note is intended for CMS internal use and distribution only

October 6, 2007

Dijet Resonance Analysis with CMSSW_1_2_0

Marco Cardaci and Benjamin Bollen

Universiteit Antwerpen, Antwerp, Belgium

Robert M. Harris

Fermilab, Batavia, IL, USA

Abstract

We report on dijet resonance studies at CMS using simulated events from CMSSW. The dijet mass distribution from QCD jet events and from dijet resonances are presented. Results from CMSSW_1_2_0 are in reasonable agreement with those from ORCA published in the Physics TDR. We estimate the statistical sensitivity to resonances of mass 0.7, 2.0 and 5.0 TeV for integrated luminosities of 10 pb⁻¹, 100 pb⁻¹, and 1 fb⁻¹. With only 10 pb⁻¹ CMS can see a 4σ signal for a 2 TeV excited quark, including statistical uncertainties only. We estimate the pseudorapidity cut on the two leading jets that provides optimal statistical sensitivity to dijet resonances is $|\eta| < 1.3$

1 Introduction

1.1 Theoretical Motivation

In the Standard Model the properties of quarks and leptons are explained in terms of basic principles rising from the nature of the electromagnetic, weak and strong interactions. Despite the beautifulness of these principles, the theory is incomplete, leaving open questions like: Why are there quark flavors? Why are quarks arranged in generations? Why are there so many different forces? How do we unify gravity with the other forces? Why is gravity so weak? Models of new particles [1] like excited quarks, axigluons, colorons, E_6 diquarks, color octet technirhos, W' , Z' , and Randall-Sundrum gravitons could give an answer to one or more of these fundamental questions.

1.2 Experimental Technique

Experiments like CMS will look for the discovery of new particles from the first day of data taking. One of the most promising channels for discovery of these particles is the high mass dijet resonance channel. All the models already mentioned produce narrow resonances decaying in two jets. In these processes all the final and initial state particles are partons (quarks, antiquarks and gluons).

The main background of a signal interaction producing two final state partons is constituted by the QCD $2 \rightarrow 2$ scattering processes.

It is natural to search for resonances using the dijet invariant mass spectrum through simple bump hunting. This approach preserves the generality which allows us to discover particles expected by one or another particular model as well as to give useful inputs to the building of new models.

1.3 This Study

The work presented in this note is a natural continuation of a previous analysis [1] which described the CMS plans to search for high mass dijet resonances and was published in the Physics TDR [2]. That study discussed the triggers we will use to do the search which were explored in detail previously [3].

The first motivation for our work is to validate the simulation of dijet resonance signals and backgrounds in CMSSW by comparing it to ORCA. We will compare the dijet resonance invariant mass shapes and the QCD differential cross section in the two simulations.

The second motivation is to produce plots that demonstrate our sensitivity for three nominal resonance masses at integrated luminosities of 10 pb^{-1} , 100 pb^{-1} and 1 fb^{-1} . We note that detailed studies were previously performed [1] to estimate our sensitivity for 100 pb^{-1} , 1 fb^{-1} , and 10 fb^{-1} , and we do not repeat those estimates here.

The third motivation is to improve the dijet resonances analysis by optimizing the $|\eta|$ cut.

2 Datasets

The data sets used in our analysis are the CMSSW Monte Carlo Samples produced by the LPC MC production group at the FermiLab Tier1. On the aim of the study of the response of the CMS detector to the dijet resonances signal, we have used:

- 4000 events of Z' at a mass of 700 GeV decaying to dijets,
- 3000 events of Z' at a mass of 2000 GeV decaying to dijets,
- 3000 events of Z' at a mass of 5000 GeV decaying to dijets;

produced and reconstructed with CMSSW_1_2_0. As in the previous analysis, the Z' has been generated with Pythia and forced to decay to u, d, s and c quarks. From these events a generic dijet invariant mass shape is obtained and if needed normalized to the cross sections anticipated by all the models considered in our analysis, which foresee a dijet resonance; a resonance that can decay to 2 jets in our analysis. All the expected cross sections are listed in table 1. Our background is mainly given by the $2 \rightarrow 2$ QCD scattering of parton interactions. To study the background we use 958,497 events divided in different p_T ranges as in table 2.

Mass (GeV)		700	2000	5000
Cross section for $ \eta < 1.0$	Q* (pb)	0.7954E+03	0.9011E+01	0.1819E-01
	Axigluon (pb)	0.3225E+03	0.5792E+01	0.1548E-01
	E_6 Diquark (pb)	0.8113E+02	0.4197E+0	0.4648E-01
	Z' (pb)	0.8858E+01	0.1813E+00	0.5501E-03
	W' (pb)	0.1461E+02	0.3494E+00	0.8717E-03
	RS Graviton (pb)	0.3573E+02	0.1828E+00	0.2637E-03

Table 1: Lowest order cross section times branching ration times acceptance for dijet resonances with $|\eta| < 1.0$ from various models. See [1].

Furthermore, on the aim of the comparison between CMSSW and ORCA, histos produced from ORCA samples have been used.

In CMSSW pile-up was not included in either the data samples or in the jet corrections. In ORCA pile-up was included in both. In both cases the resulting corrected jets are at the particle level before any pile-up, and so are directly comparable. Also the CMSSW results use the Scheme B cell thresholds while ORCA used Scheme N [4].

sample i	\hat{p}_T (GeV)	Events N_i	σ_i (mb)
1	0 - 15	25277	5.52E+01
2	15 - 20	50100	1.46E+00
3	20 - 30	99465	6.32E-01
4	30 - 50	98420	1.63E-01
5	50 - 80	100590	2.16E-02
6	80 - 120	48558	3.08E-03
7	120 - 170	50195	4.94E-04
8	170 - 230	49352	1.01E-04
9	230 - 300	49253	2.45E-05
10	300 - 380	30551	6.24E-06
11	380 - 470	50251	1.78E-06
12	470 - 600	50079	6.83E-07
13	600 - 800	29748	2.04E-07
14	800 - 1000	30193	3.51E-08
15	1000 - 1400	27441	1.09E-08
16	1400 - 1800	30116	1.06E-09
17	1800 - 2200	27125	1.45E-10
18	2200 - 2600	30178	2.38E-11
19	2600 - 3000	30321	4.29E-12
20	3000 - 3500	29920	8.44E-13
21	3500 - 7000	21364	1.08E-13

Table 2: QCD Dataset from CMSSW_1_2_0. For each sample number i we list the \hat{p}_T range, the number of events generated, and the cross section. See text for how these numbers are used to calculate the QCD cross section.

3 Software

The analysis code we used is in the CMSSW CVS repository in `/UserCode/SUSYBSMsandbox/wg4/Dijet/marco`. The basic code to produce histograms is `JetPlotsExample.cc` and `JetPlotsExample.h`. These files replace corresponding files in the standard jet analysis example from the CMSSW workbook: `JetPlotsExample` in the package `RecoJets/JetAnalyzers`. They define an `EDAnalyzer` which produces the histogram files. For QCD the histograms are produced separately for each \hat{p}_T bin, and for dijet resonances the histograms are produced separately for each resonance mass. The root scripts, described in the file `README`, use the histogram files and cross section weights to produce the QCD and dijet resonance figures in this analysis note.

4 Dijet Mass Distributions

We made plots of the dijet invariant mass for two jet algorithms, two types of inputs, and with jet corrections. The algorithms were midpoint cone with cone size $R = 0.5$ and iterative with cone size $R = 0.5$; they were very similar so we chose to only show Iterative cone jets in this note for the simplest comparison with ORCA. The inputs were either CaloTowers (CaloJets), or HepMCparticles (GenJets). For the cone algorithms, CMSSW_1_2_0 jet corrections from MCJet [5] were applied to form corrected CaloJets (CorJets). In all cases we form the dijet invariant mass from the first two jets in the collection, the leading jets for p_T ordered jet collections, and we require each leading jet have $|\eta| < 1.0$ unless otherwise stated.

4.1 QCD background

The differential cross section for the QCD background is determined by combining the samples in table 2 appropriately weighted by the cross section and events listed. In detail, the differential cross section, $d\sigma/dm$, in a bin of dijet mass is calculated from the contributions of all the \hat{p}_T samples by the equation

$$\frac{d\sigma}{dm} = \sum_{i=1}^{21} \frac{n_i \sigma_i}{N_i \Delta m} \quad (1)$$

where n_i is the number of events in the bin of dijet mass originating from \hat{p}_T sample i , σ_i is the cross section for \hat{p}_T sample i , N_i is the total number of events generated in \hat{p}_T sample i , and Δm is the width of the dijet mass bin. We use the same mass bins as the previous analysis [1] as discussed in the next section.

In Figure 1 we show the QCD differential cross section for GenJets, CaloJets and corrected CaloJets. The bin edges, cross section values, and MC statistical errors are listed in table 3 for future reference. The cross section for CaloJets is much less than the cross section for GenJets, because the CaloJet energy is much lower due to CMS calorimeter response, and the entire CaloJet distribution is essentially shifted to lower mass with respect to the GenJet distribution. The jet corrections are designed to correct the energy of a CaloJet back to the energy of the corresponding GenJet on average. As a result, the cross section for corrected CaloJets is similar to the cross section for GenJets.

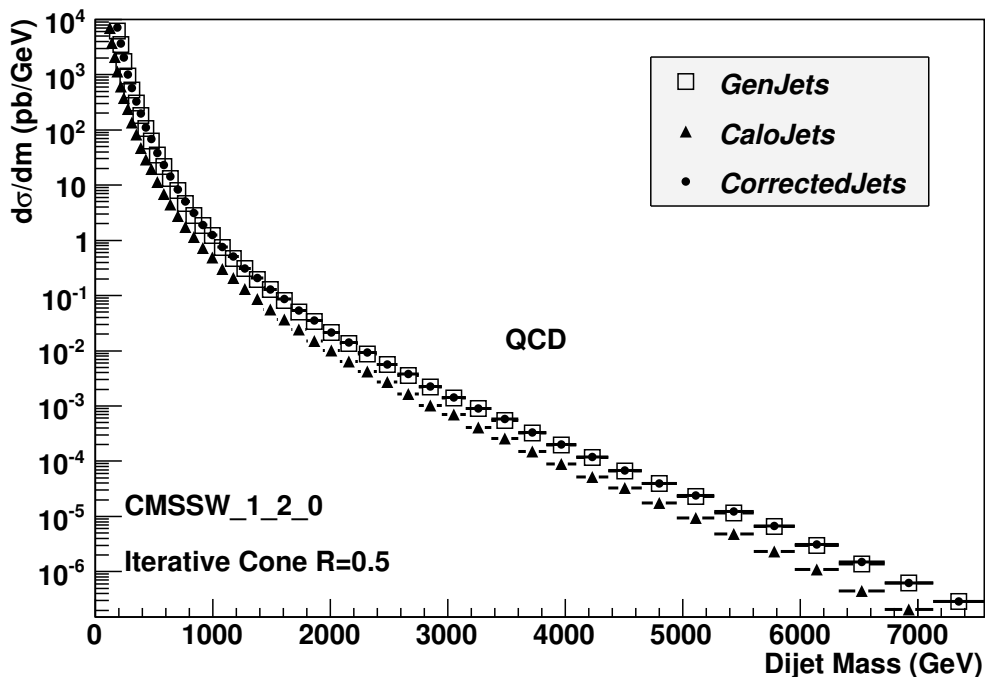


Figure 1: QCD differential cross section as a function of dijet invariant mass for GenJets, CaloJets, and corrected CaloJets.

Bins		GenJets		CaloJets		CorJets	
Low Edge (GeV)	Width (GeV)	Xsec (pb/GeV)	Error (pb/GeV)	Xsec (pb/GeV)	Error (pb/GeV)	Xsec (pb/GeV)	Error (pb/GeV)
176.208	25.35	6230.54	165.606	1135.88	39.7205	7095.88	234.455
201.558	27.709	3520.52	103.593	607.806	19.1209	3628.44	110.304
229.267	30.202	1745.16	55.7613	374.299	11.5163	2057.76	66.9814
259.469	32.837	946.724	30.1296	238.055	8.26914	1013.92	35.7433
292.306	35.623	530.676	17.8358	135.6	3.74459	575.302	20.2388
327.929	38.564	308.194	9.52522	82.6966	2.81829	325.685	10.0813
366.493	41.671	182.429	5.0275	47.4103	1.25388	197.084	7.07505
408.164	44.948	106.265	2.8561	29.2787	0.806616	110.164	3.31332
453.112	48.408	62.3932	2.10753	19.6777	0.529353	67.7506	2.36817
501.52	52.056	34.9452	0.904957	11.2761	0.299	38.1676	1.03521
553.576	55.905	21.6299	0.533114	6.84988	0.187001	22.9012	0.635682
609.481	59.961	13.2723	0.407858	4.42505	0.122353	14.2555	0.398322
669.442	64.237	8.04574	0.208832	2.75349	0.0706298	8.35325	0.230471
733.679	68.743	4.65967	0.128876	1.74294	0.041263	5.05407	0.140335
802.422	73.489	2.82766	0.0745046	1.13647	0.0254853	3.12702	0.0885729
875.911	78.489	1.8693	0.0443728	0.727467	0.0154331	1.90581	0.0486402
954.4	83.75	1.22003	0.0366235	0.485326	0.0104687	1.23545	0.0297051
1038.15	89.2999	0.735903	0.015389	0.304899	0.00667743	0.763632	0.0166184
1127.45	95.13	0.464107	0.0090216	0.207286	0.00451574	0.505249	0.0109348
1222.58	101.26	0.311264	0.00710543	0.130636	0.00315487	0.311324	0.00688451
1323.84	107.73	0.194982	0.00415676	0.0863515	0.00221818	0.206268	0.00476263
1431.57	114.52	0.128931	0.00296396	0.0557825	0.00144018	0.127736	0.00300978
1546.09	121.67	0.0816044	0.00205769	0.0368266	0.000947805	0.0856802	0.00219033
1667.76	129.19	0.0498288	0.0012685	0.0240253	0.000634211	0.053064	0.00136085
1796.95	137.08	0.0338663	0.000859646	0.0151729	0.00038339	0.0350776	0.000909819
1934.03	145.4	0.0212371	0.000563268	0.0101689	0.000270564	0.0216121	0.000568529
2079.43	154.12	0.0135589	0.000342808	0.0063538	0.000167948	0.0140688	0.000374959
2233.55	163.31	0.0087951	0.000226432	0.00421239	0.000114512	0.00921438	0.000252592
2396.86	172.95	0.0055904	0.000147664	0.00269539	7.54368e-05	0.0056144	0.000149737
2569.81	183.08	0.00356572	9.98124e-05	0.00165136	4.76605e-05	0.00376091	0.000103029
2752.89	193.72	0.00219261	6.1252e-05	0.00103095	3.07408e-05	0.00226809	6.45224e-05
2946.61	204.91	0.00138634	3.94669e-05	0.0006948	2.10842e-05	0.00141281	4.08883e-05
3151.52	216.64	0.000892097	2.60676e-05	0.000410783	1.18865e-05	0.000893011	2.66554e-05
3368.16	228.98	0.000551004	1.68574e-05	0.000258583	7.3132e-06	0.000575467	1.82693e-05
3597.14	241.93	0.000326153	9.57556e-06	0.000149933	3.27718e-06	0.000333011	9.67375e-06
3839.07	255.52	0.000197919	5.2081e-06	8.84026e-06	2.12847e-06	0.0002008	6.05387e-06
4094.59	269.79	0.000116352	2.97595e-06	5.2033e-06	1.25522e-06	0.000120327	2.73859e-06
4364.38	284.77	6.71595e-05	1.64709e-06	3.2433e-05	8.70349e-07	6.74338e-05	1.68441e-06
4649.15	300.49	3.97971e-05	1.02349e-06	1.73912e-05	4.55174e-07	3.94103e-05	9.6517e-07
4949.64	317	2.27664e-05	5.99011e-07	9.29762e-06	2.16129e-07	2.394e-05	7.11255e-07
5266.64	334.3	1.15444e-05	2.72508e-07	4.84632e-06	1.22788e-07	1.21597e-05	3.2555e-07
5600.94	352.47	6.63961e-06	1.86045e-07	2.2938e-06	6.20523e-08	6.73573e-06	1.70832e-07
5953.41	371.53	3.00695e-06	7.99895e-08	1.09457e-06	3.05291e-08	3.07937e-06	8.5573e-08
6324.94	391.53	1.38764e-06	3.70904e-08	4.50902e-07	1.31544e-08	1.49843e-06	4.52914e-08
6716.47	412.49	6.23733e-07	1.77658e-08	2.06498e-07	6.19593e-09	6.27062e-07	1.82275e-08
7128.96	434.04	2.89385e-07	8.76233e-09	8.26654e-08	3.29172e-09	2.86332e-07	9.27392e-09

Table 3: QCD Cross Section: For each bin of dijet mass, the lower bin edge, bin width, cross section and statistical error are shown for GenJets, CaloJets and corrected CaloJets. This table requires each leading jet have $|\eta| < 1.0$ and corresponds to the curves shown in Fig 1.

An important test of the cross section weight procedure is whether the resulting dijet cross section is smoothly falling. In Figure 2 we show that we are able to fit the distribution with a four parameter function between a mass of 0.3 and 7 TeV and get a reasonable χ^2 of 39 for 36 degrees of freedom, an acceptable 32% probability. The fit function used

$$\frac{d\sigma}{dm} = p_0 \frac{(1 - \frac{m}{\sqrt{s}} + p_3(\frac{m}{\sqrt{s}})^2)^{p_1}}{(m/\sqrt{s})^{p_2}} \quad (2)$$

is identical to that employed by CDF [6] to model the QCD background when searching for dijet resonances. It could also be used by CMS for a similar purpose.

Fit on QCD differential cross section at Corrected Level

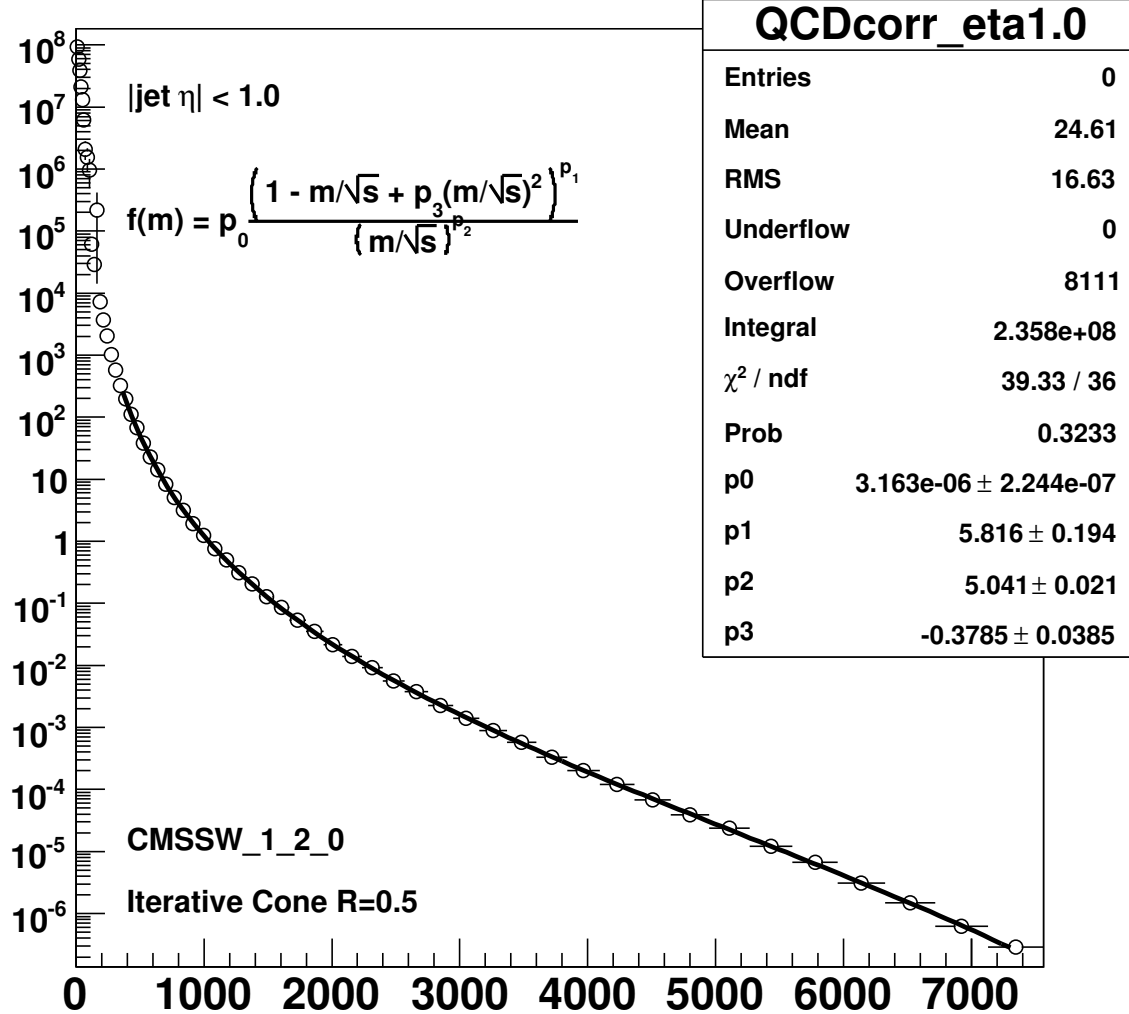


Figure 2: The QCD differential cross section fit to a smooth parameterization with 4 parameters.

4.2 Dijet Resonance Shapes

We can ideally decompose the shape of the dijet invariant mass distribution for narrow dijet resonances into two parts: a first Gaussian part, due to intrinsic jet energy resolution and a second low mass tail part due mainly to radiation of the final state partons. For a 5 TeV Z' there is also a contribution on the tail from the parton distributions. This is demonstrated in Figure 3 where we can see a very long low mass tail at generator level for the 5 TeV Z' resonance but a smaller one for the 2 TeV and 700 GeV Z' resonances. This affects both the particle level and calorimeter level jets. The size of this effect depends on the width of the narrow resonance and the kind of

partons in the initial state. We can see that the distributions at CaloJets level peak at lower mass than GenJets one. This is due to low calorimeter response as discussed above for the QCD sample. The correction on the CaloJets distribution restore the peak of the distribution to the nominal mass value, making the CorJets distribution very similar to the GenJets distribution.

In the previous analysis [1] a fit to the Gaussian part of the distribution was used to obtain an estimate of the dijet mass resolution. The width used for each bin was chosen to be of size 1σ to optimally resolve a resonance bump on the spectra. For best comparison with the previous analysis, we have used that same bin width throughout this analysis.

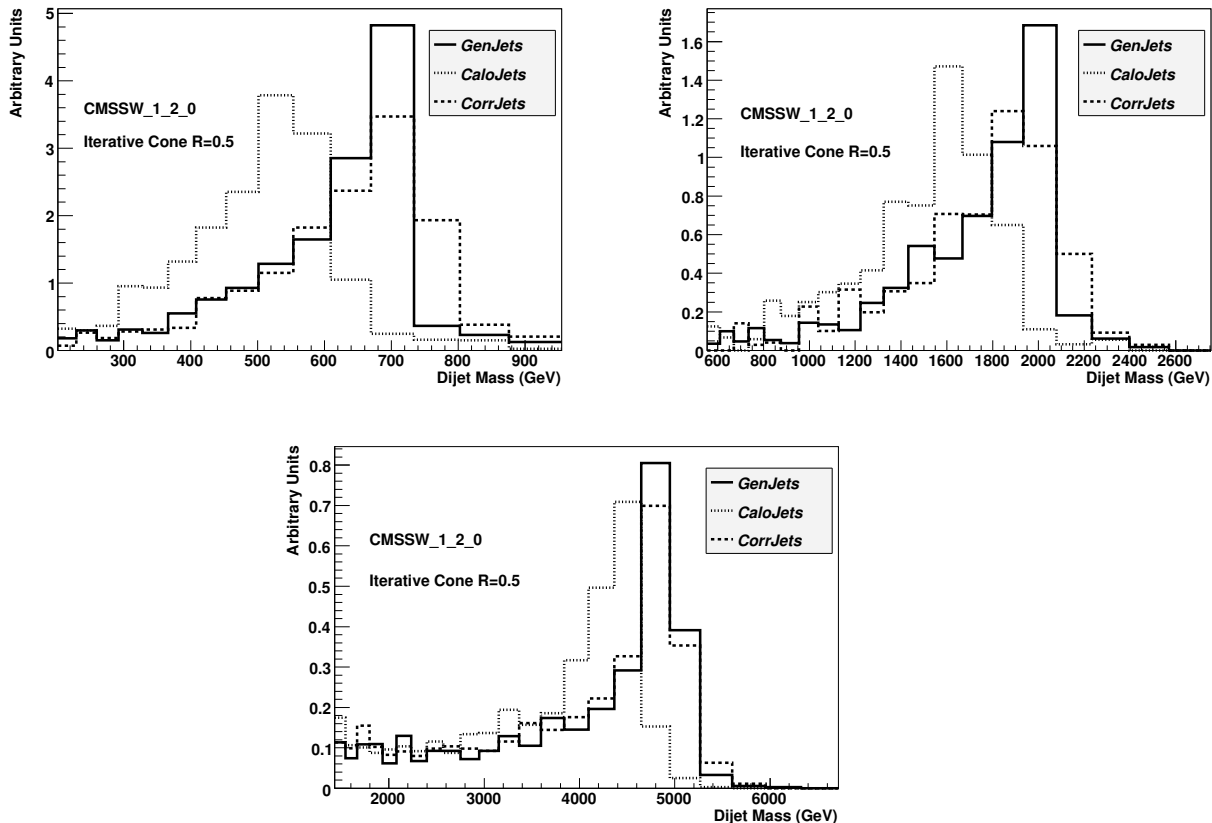


Figure 3: Dijet invariant mass from a Z' of mass 700 GeV (top left plot), 2000 GeV (top right plot), and 5000 GeV (bottom plot). Histograms are shown for GenJets, CaloJets, and corrected CaloJets.

5 Dijet Resonances and QCD background in CMSSW and ORCA

In this section we will present a comparison of the dijet resonances and of the QCD background in CMSSW and ORCA. This will include a direct comparison of the dijet resonance shapes for 3 mass points at generator and corrected level and of the QCD differential cross sections at generator and corrected level.

In Figure 4 we can see the dijet invariant mass plots made with CMSSW and ORCA. The plots coming from the different CMS software are normalized to 1 and superimposed to allow an easier comparison. The agreement between the two simulations is quite good and allow us to be confident on the studies performed in ORCA and to go further in our analysis with CMSSW based simulation.

In Figure 5 we can see the fractional difference between QCD cross sections in CMSSW and ORCA for corrected CaloJets and for GenJets. The differences between the CMSSW and ORCA simulations for Corrected CaloJets are similar to the differences for GenJets. The cause of the difference is not fully understood. Known differences between the two CMSSW and ORCA simulations include the following effects which may be partially responsible

- GenJets from CMSSW include neutrinos and muons while GenJets from ORCA did not. This makes the

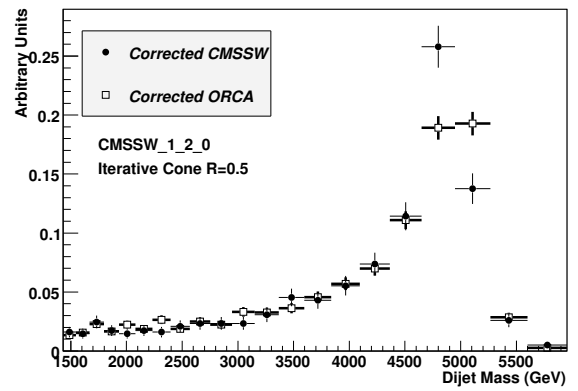
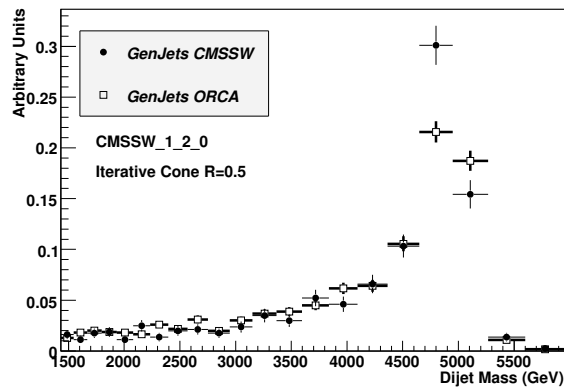
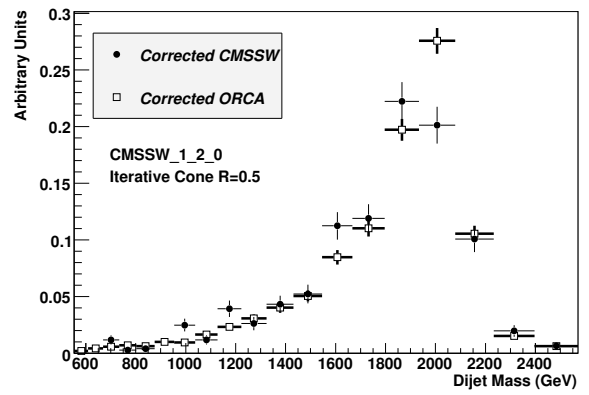
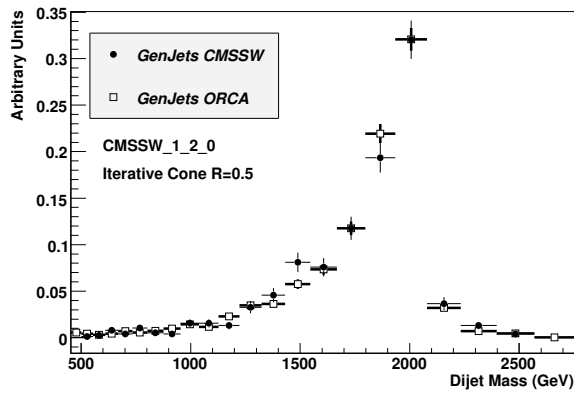
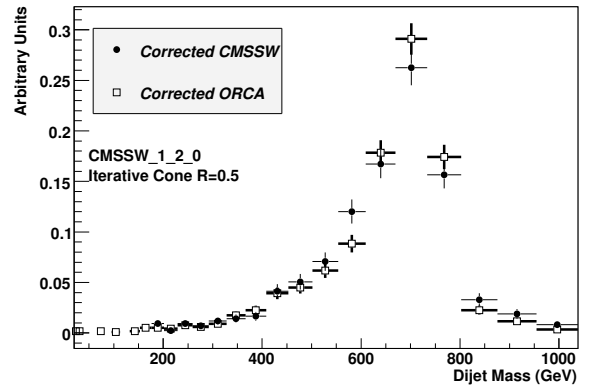
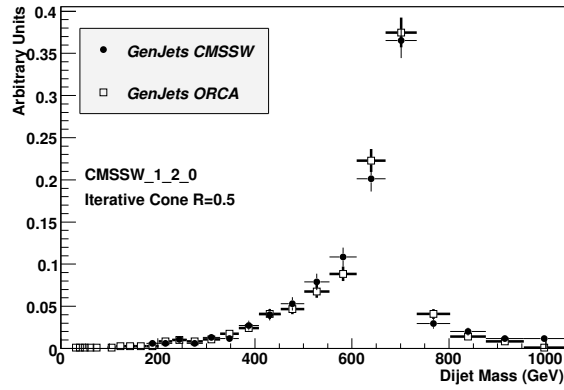


Figure 4: Dijet invariant mass from CMSSW and ORCA is compared for a Z' of mass 700 GeV (top plots), 2000 GeV (middle plots), and 5000 GeV (bottom plots), for GenJets (left plots) and corrected CaloJets (right plots).

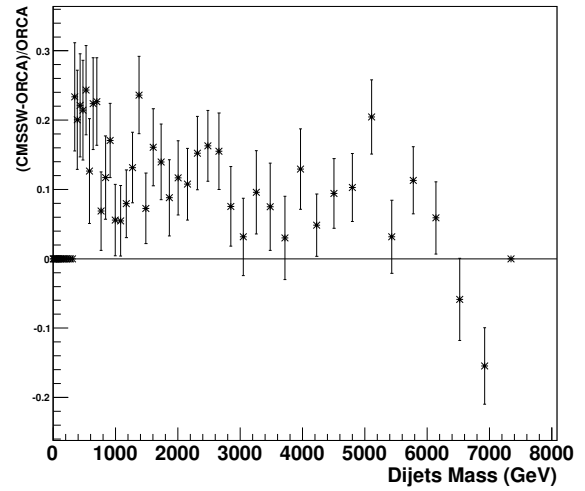
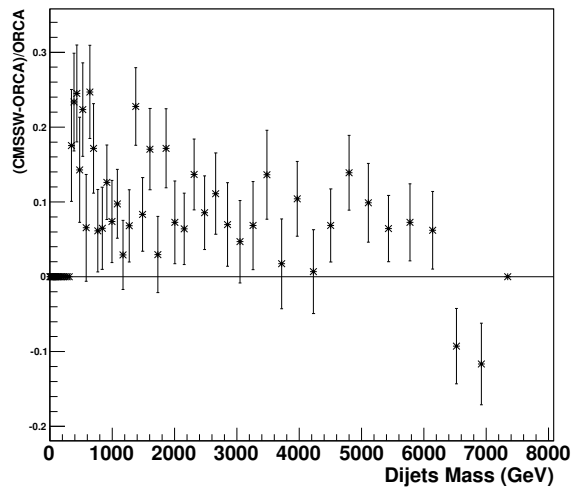


Figure 5: Fractional difference between QCD cross sections in CMSSW and ORCA for GenJets (left plot) and corrected CaloJets (right plot)

GenJet energy slightly larger and the cross section at a fixed GenJet dijet mass larger.

- Underlying event tune in CMSSW is different than in ORCA.
- Corrected calorimeter response in CMSSW may be somewhat different than ORCA.

The two QCD distributions are close enough for our current study.

6 Signal Compared to Background

In Figure 6 we compare the cross section for an excited quark dijet resonance signal to the statistical uncertainties expected on the QCD dijet background for three luminosity scenarios: 10pb^{-1} , 100pb^{-1} and 1fb^{-1} . The normalization of the excited quark signal came from our lowest order calculation in table 1 and the shape of the excited quark signal comes from the CMSSW simulation of dijet resonances for corrected CaloJets in Figure 3. The statistical uncertainties on the QCD background was obtained for the expected rates of corrected CaloJets, coming from the cross sections in Figure 1 and table 3 multiplied by the luminosities and trigger prescales discussed previously [1].

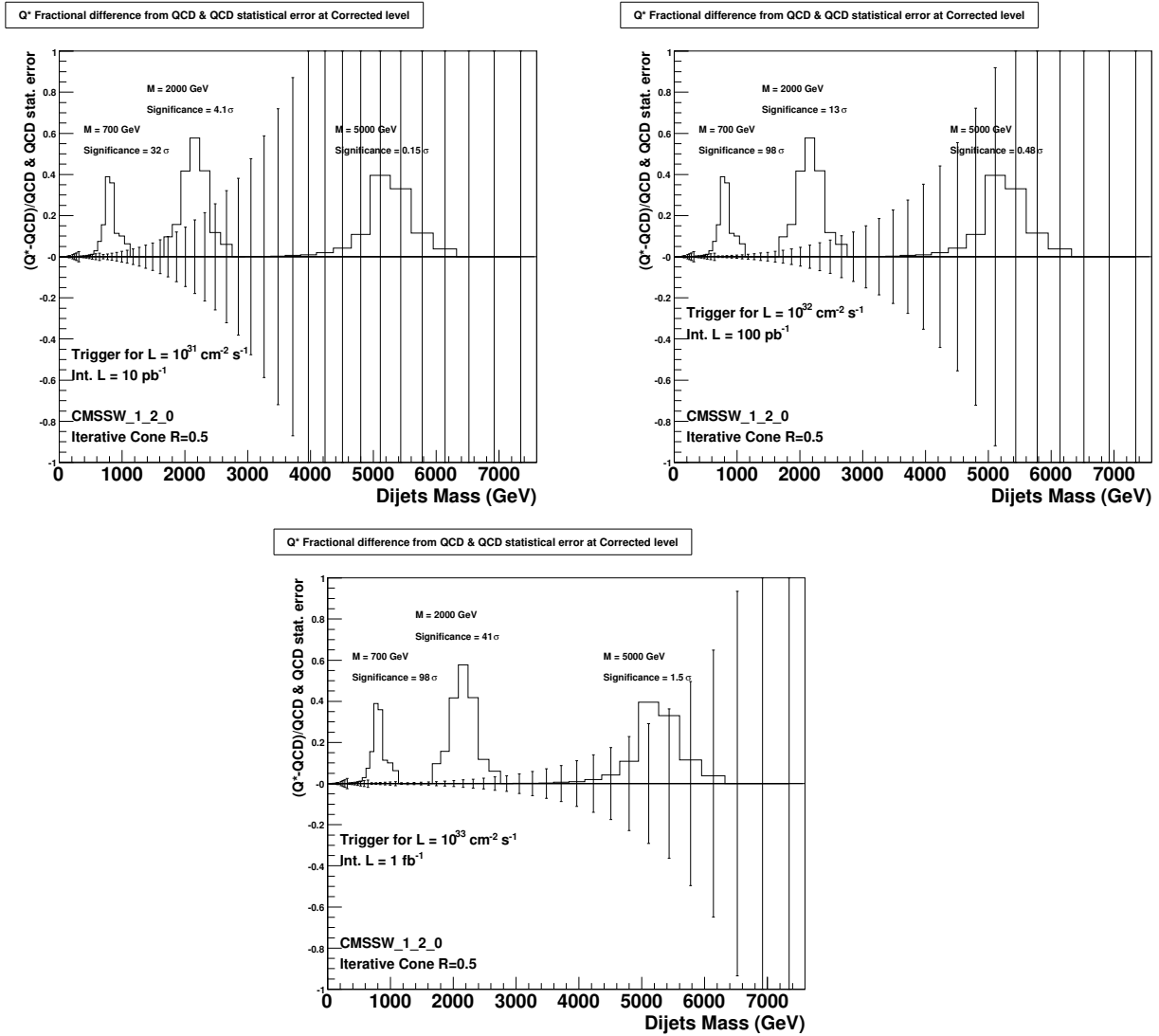


Figure 6: Fractional difference between an excited quark signal and the QCD background compared to the QCD statistical error for an integrated luminosity of 10pb^{-1} (top left plot), 100pb^{-1} (top right plot) and 1fb^{-1} (bottom plot).

Figure 6 shows we will be sensitive to an excited quark signal up to many TeV. With only 10pb^{-1} we can see a 2 TeV excited quark signal beginning to emerge above our statistical error bars with a total significance of 4.1σ , neglecting systematic uncertainties. With 100pb^{-1} the same 2 TeV signal has a convincing significance of 13σ . In Figure 6 we list the total statistical significance for an excited quark signal at each resonance mass next to the mass peak on each plot. This total significance comes from summing the bin-by-bin significances in quadrature. For example in Figure 7 we show the bin-by-bin significance of the excited quark signal for an integrated luminosity of 1fb^{-1} . The total significance for the signal is then found by summing the bin-by-bin significance in quadrature for the complete resonance. We will use this simple and robust technique for estimating statistical significance in

Significance at Corrected Level

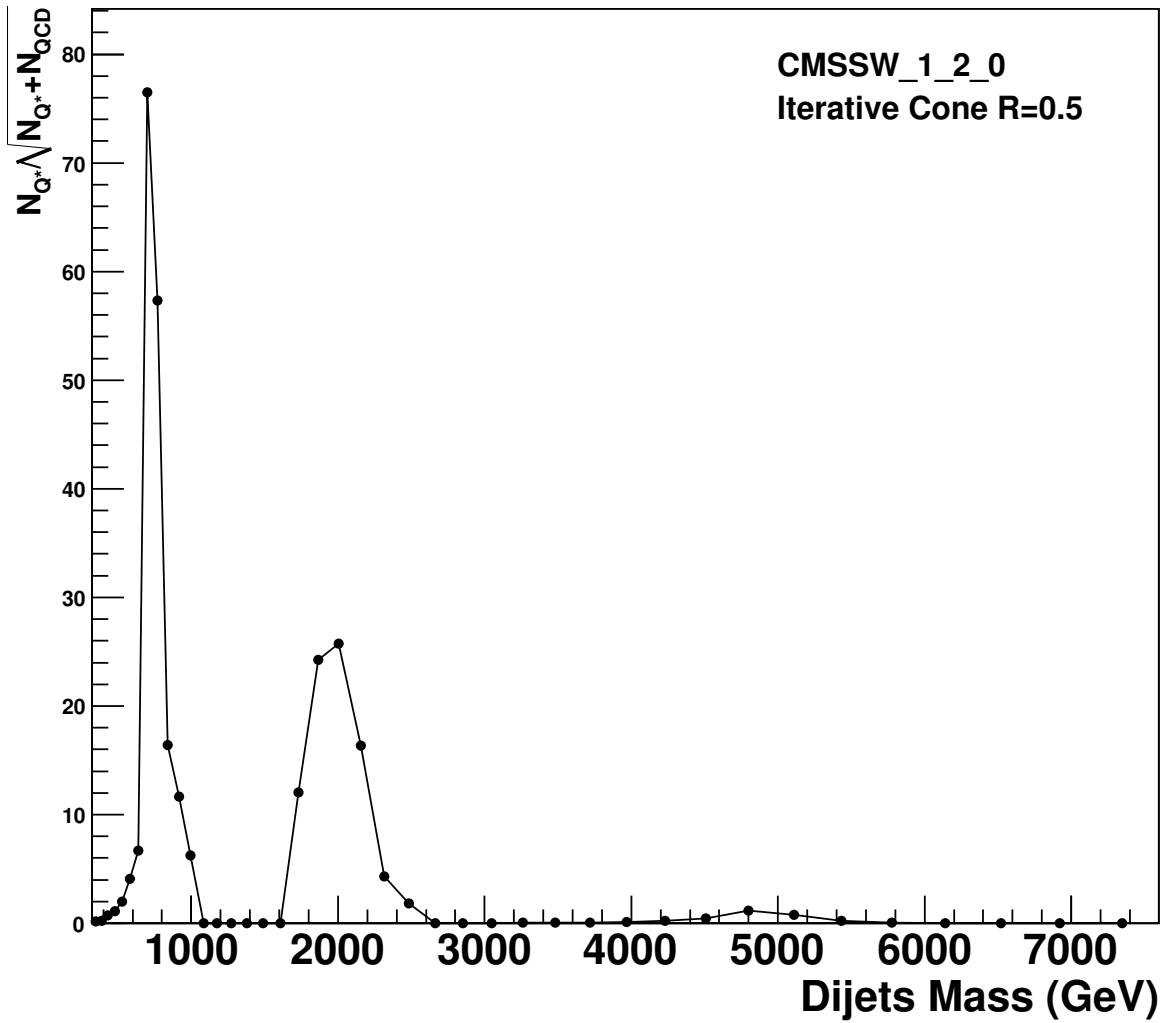


Figure 7: The bin by bin statistical significance of an excited quark signal compared to the QCD background as a function of dijet mass in units of standard deviations (σ) for 1 fb^{-1} of integrated luminosity.

7 $|\eta|$ cut optimization

The dijet resonance analysis presented so far required each leading jet to be in the region $|\eta| < 1.0$, just like in the Physics TDR [2]. This cut was inherited from the Tevatron, but it was never optimized for CMS. Here we will estimate the optimal value of this cut for statistical sensitivity to dijet resonance signals.

In Figure 8 we show the differential cross section as a function of dijet mass for the QCD background and a dijet resonance signal for 36 values of the $|\eta|$ cut, varying from $|\eta| < 0.5$ to $|\eta| < 4.0$ in steps of 0.1. The signal shape is from Figure 3 and the signal normalization is from our lowest order calculation for an excited quark for the value $|\eta| < 1$ multiplied by the relative signal acceptance, R , of the given $|\eta|$ cut compared to the $|\eta| < 1$ cut in the dijet resonance simulation

$$R = \frac{N(|\eta| < \text{cut})}{N(|\eta| < 1)} \quad (3)$$

where N is the number of events measured in the resonance simulation with the particular $|\eta|$ cut. The background shape and normalization is from the QCD simulation with the given $|\eta|$ cuts. As we relax the eta cut from the default value of $|\eta| < 1.0$ to higher values, up to $|\eta| < 4.0$, the QCD background cross section increases by nearly three orders of magnitude. This is because QCD is dominated by t-channel scattering, simple Rutherford-like scattering, which peaks in the forward direction. In contrast the dijet resonance signal increases only slightly as we relax the $|\eta|$ cut from 1 to 4, because dijet resonance production is an s-channel process, which is always more isotropic and hence more centrally produced than a t-channel process. Thus if the $|\eta|$ cut is completely relaxed we expect the significance of the signal over the QCD background to decrease dramatically. Conversely if the $|\eta|$ cut is tightened to very small values then we will have very few signal events and we again expect the significance of the signal to be low. Somewhere in between we expect an optimal value.

We note that the precise rate as a function of $|\eta|$ for the resonances will depend on the detailed helicity of the resonance decay to dijets: the resonance spin, and whether the resonance decays to quarks (fermions) or gluons (bosons). However, compared to the t-channel pole of QCD, which increases the rate dramatically at high $|\eta|$, all s-channel resonances are roughly isotropic in rate vs. $|\eta|$. Here we have done the optimization for the angular distribution of a spin 1 particle (Z') decaying to quarks. We expect the exact value for the optimization to be slightly different for other kinds of dijet resonances from spin arguments alone.

In Figure 9 we show the total statistical significance of the signal compared to the background as a function of the $|\eta|$ cut for an integrated luminosity of 1 fb^{-1} . The significance is calculated by summing in quadrature the bin-by-bin statistical significance over all the bins of the resonance. The significance is calculated independently for each of three resonance masses, 0.7, 2, and 5 TeV. An $|\eta|$ cut of 1.3, shown by a vertical line in Figure 9, maximizes the significance for a 2 TeV resonance, and has a very similar significance as the maximum significance cut for a 0.7 and 5 TeV resonance as well. It is likely the best single value for an $|\eta|$ cut for this analysis, and we recommend its use in the future.

While we recommend a single cut at $|\eta| < 1.3$, we also note from Figure 9 that as the resonance mass increases the $|\eta|$ cut which maximizes the significance decreases from $|\eta| < 1.5$ at $M = 0.7 \text{ TeV}$ to $|\eta| < 1.0$ at $M = 5 \text{ TeV}$. This is because the resonances at $M = 0.7 \text{ TeV}$ can have a significant boost along the beam, because the proton-proton collisions are at relatively low fractional momentum ($x \sim 0.05$) and it is easy to find two partons with very different values of x around this low x value, and this boost increases the signal fraction at high η values. At a mass of $M = 5 \text{ TeV}$ the fractional momentum of each proton is much higher ($x \sim 0.4$), and it is much more difficult to find two widely varying values of x around this already high median value. A large fraction of the energy of the proton went into creating the massive resonance and there is very little left over to provide boost to such a massive object: the resonance stays at low $|\eta|$. Although a sliding cut appears to be optimal from a statistical point of view, and appears to be well motivated from the physics, we do not recommend a sliding cut for the first resonance searches at CMS for the following reasons. A sliding cut might introduce a mass dependence into the analysis which would increase the chances of generating spurious signals, particularly if the eta cut allowed jets outside the barrel for one mass region but required them all to be inside the barrel for another mass region. The simpler $|\eta| < 1.3$ cut will provide a single uniform region of calorimeter response in the barrel and better control the systematic uncertainties. Further, at this point we do not want to tune the analysis too much on this single resonance hypothesis, since the exact angular dependence will depend on the exact helicity of the resonance. We want to keep the search generic, and we are just using this resonance model to guide us toward what is the general region of the calorimeter we should use for the analysis. We note that in the future it may be possible to increase our sensitivity slightly by going to a sliding cut, assuming the systematics are well understood, but at this point we can only recommend a single cut at $|\eta| < 1.3$.

Differential cross section at corrected level

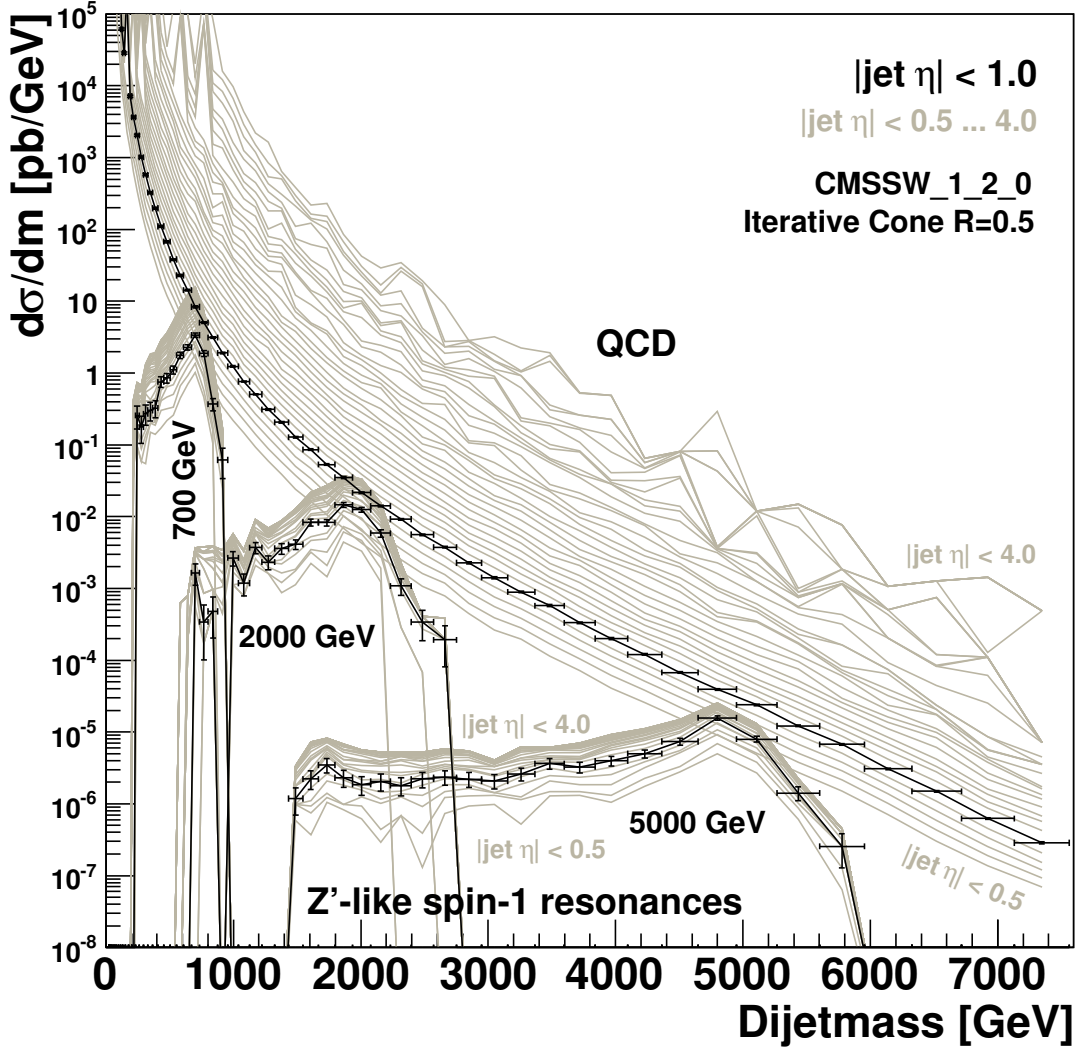


Figure 8: The cross section for a dijet resonance signal (see text) and the QCD background as a function of dijet mass is shown for the cut $|\eta| < 1$ (points and dark curves) and for various values of the $|\eta|$ cut between 0.5 and 4.0 (light curves).

Measure of significance versus η -cut

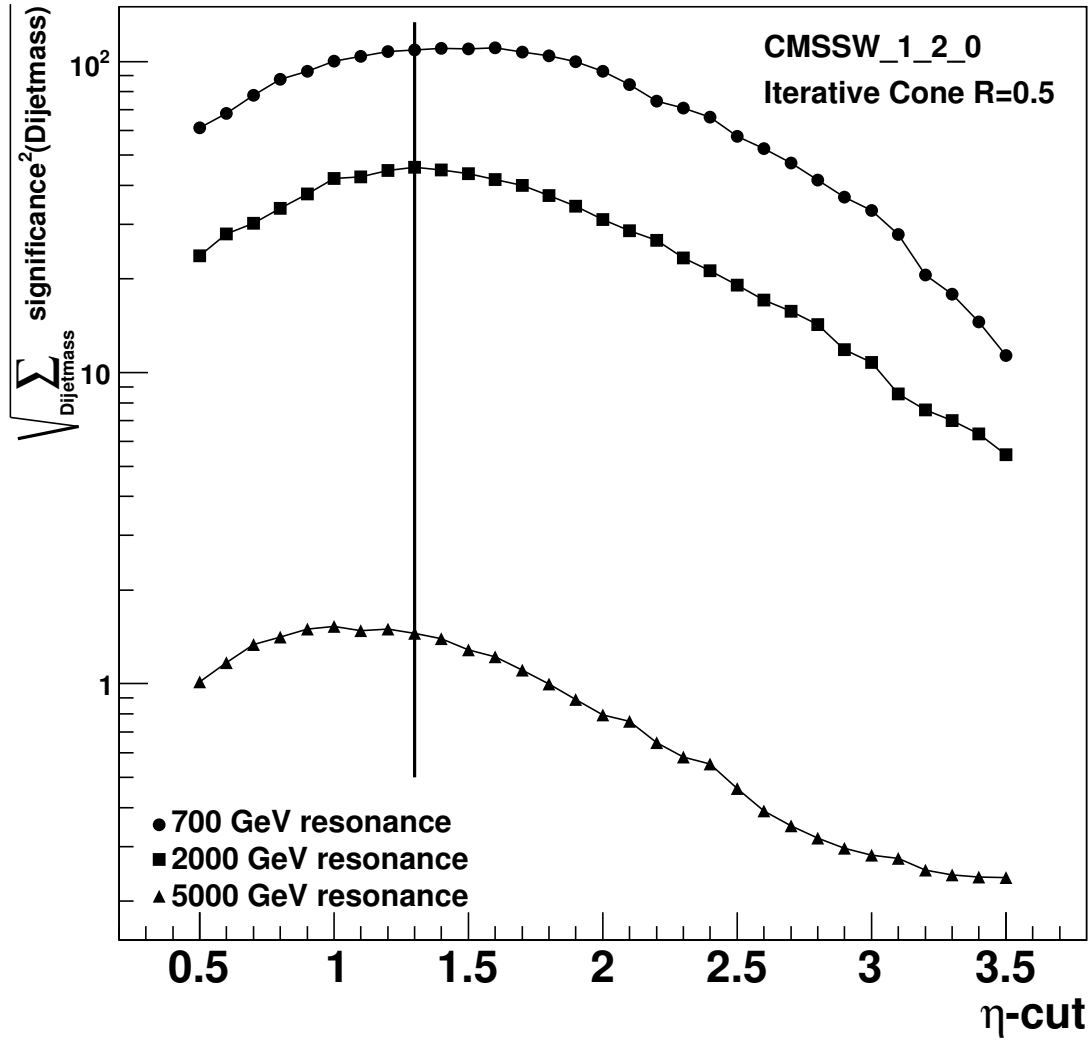


Figure 9: The statistical significance of a dijet resonance signal (see text) as a function of the $|\eta|$ cut for 1 fb^{-1} of integrated luminosity is shown for a resonance of mass 700 GeV (triangles), 2000 GeV (squares) and 5000 GeV (circles).

8 Conclusion

We have repeated the basic plots in the dijet resonance analysis of Physics TDR II using CMSSW 1.2.0, and we have compared some basic distributions between ORCA and CMSSW 1.2.0. We find reasonable levels of agreement.

We have estimated the statistical sensitivity to resonances of 0.7, 2.0 and 5.0 TeV for integrated luminosities of 10 pb^{-1} , 100 pb^{-1} , and 1 fb^{-1} . With only 10 pb^{-1} CMS can see a 4σ signal for a 2 TeV excited quark in the absence of systematic uncertainties.

We have estimated the pseudorapidity cut on the two leading jets that provides optimal statistical sensitivity to dijet resonances in the presence of the QCD background. We recommend a single cut at $|\eta| < 1.3$, within the CMS barrel, be used to search for dijet resonances.

References

- [1] K. Gumus, N. Akchurin, S. Esen and R. Harris, **CMS Note 2006/070**, "CMS Sensitivity to Dijet Resonances", May 2006.
- [2] CMS Collaboration, **CERN-LHCC-2006-021; CMS-TDR-008-2; J. Phys. G: Nucl. Part. Phys. 34 995-1579**, *CMS Physics Technical Design Report Volume II (PTDR2) : Physics Performance.*, August 2006.
- [3] S. Esen and R. Harris, **CMS Note 2006/069**, "Jet Triggers and Dijet Mass", May 2006.
- [4] M. Zielinski et al., **CMS-Note - 2006/020**, "Calorimeter Cell Energy Thresholds for Jet Reconstruction in CMS".
- [5] M. Vazquez Acosta et al., **CMS IN - 2007/053**, "Jet and MET Performance in CMSSW_1.2.0", September 2007.
- [6] F. Abe et al. (CDF Collaboration), "Search for New Particles Decaying to Dijets at CDF", **Phys. Rev. D55: 5263-5268 (1997)**, **hep-ex/9702004**.